

Thermally activated dynamics of spontaneous perpendicular vortices tuned by parallel magnetic fields in thin superconducting films

Milind N. Kunchur* and Manlai Liang

Department of Physics and Astronomy, University of South Carolina, Columbia, South Carolina 29208, USA

Alex Gurevich

Department of Physics, Old Dominion University, Norfolk, Virginia 23529, USA

(Received 9 April 2012; revised manuscript received 3 July 2012; published 24 July 2012)

We report magnetotransport measurements on a superconducting molybdenum-germanium (MoGe) film of thickness $d = 50$ nm in parallel magnetic fields and show evidence of a transition from a Meissner state to a resistive state of spontaneous perpendicular vortices generated by thermal fluctuations above a certain temperature $T > T_v(B)$. Here T_v appears to match the vortex core explosion condition $d \approx 4.4\xi(T_v)$, where ξ is the coherence length. For $T > T_v$, we observed that a nonlinear current-voltage (I - V) response (Ohmic at low currents and the power law $V \propto I^\beta$ at higher I) is exponentially dependent on B^2 . We propose a model in which the resistive state at $T > T_v$ is due to thermally activated hopping of spontaneous perpendicular vortices tuned by the pairbreaking effect of the parallel B .

DOI: [10.1103/PhysRevB.86.024521](https://doi.org/10.1103/PhysRevB.86.024521)

PACS number(s): 74.25.Wx, 74.25.Ha, 74.25.Op, 74.25.Uv

I. INTRODUCTION

The mixed state of Abrikosov vortices in type II superconductors exists between the lower and upper critical magnetic fields, B_{c1} and B_{c2} . In a film of thickness d smaller than the magnetic penetration depth $\lambda(T)$ but larger than the coherence length $\xi(T)$, the lower critical field $B_{c1}^{\parallel} = (2\phi_0/\pi d^2) \ln(d/\xi)$ parallel to the film surface can well exceed the bulk B_{c1} .¹ As d decreases the vortex currents get squished by the film surfaces, so the vortex core becomes unstable and extends all the way across the film if the thickness becomes smaller than $d = 4.4\xi(T_v)$.² Such a “core explosion” transition of a vortex into a phase slip center can occur in thin films at temperatures $T > T_v$ because the coherence length $\xi(T) = \xi_0(1 - T/T_c)^{-1/2}$ diverges at the critical temperature T_c . The behavior of mesoscopic vortex structures in confined geometries has attracted much attention both experimentally³ and theoretically.^{4,5}

Thermal fluctuations can radically change the behavior of vortices in thin films in a parallel field B . For $B < B_{c1}$, parallel vortices are expelled, which would usually imply the Meissner state. However, at $T > T_v$ a thin film can be in a resistive state if short vortices perpendicular to the film surface are spontaneously generated by thermal fluctuations, the energy of such vortices $\simeq d\phi_0^2/4\pi\mu_0\lambda^2$ being of the order of $k_B T$. Perpendicular vortices can appear either through the Berezinskii-Kosterlitz-Thouless (BKT) unbinding of vortex-antivortex pairs or through the nucleation of single vortices at the film edge (unbinding from their antivortex images that then hop across the bridge).⁶ Here a parallel magnetic field can be used to tune this transition, as will be shown below.

In this work we report transport measurements on amorphous MoGe films which are a good model system for investigating intrinsic flux dynamics because of their low bulk pinning and isotropic nature.^{7,8} We observed a clear transition to a thermally activated resistive state due to hopping of spontaneous perpendicular vortices, with the dynamics tuned by the pairbreaking effect of the *parallel* magnetic field. The latter is unusual because a parallel magnetic field

does not interact with perpendicular vortices in the standard London theory. This transition was observed at T close to the core explosion transition temperature $T \approx T_v$, above which the resistance becomes strongly dependent on the parallel magnetic field.

II. EXPERIMENTAL METHODS

The electrical transport measurements were made both using continuous dc signals (detected with standard digital voltmeters/nanovoltmeters) and using pulsed signals (made with an in-house built pulsed current source, preamplifier circuitry, and a LeCroy model 9314A digital storage oscilloscope). The pulse durations are on the order of 1 μ s, and the pulse repetition frequency is about 1 Hz, which reduces macroscopic heating of the film.

The cryostat was a Cryomech PT405 pulsed-tube closed-cycle refrigerator that went down to about 3.2 K. It was fitted inside a 1.3-Tesla GMW 3475-50 water-cooled copper electromagnet mounted on a calibrated turntable. Calibrated cernox and Hall sensors monitored T and B , respectively. The accuracy of the in-film-plane alignment of the magnetic field was $\theta = 0 \pm 0.025^\circ$. In the data section below we show R vs. θ curves in the resistive state (R is strongly influenced by the pairbreaking effect of the parallel field, which depends sensitively on the alignment). This allows an accurate zero adjustment of the in-film-plane angle. We will see below that R has an exponential dependence on B^2 , consistent with a pairbreaking scenario; on the other hand, if \mathbf{B} were slightly tilted so as to produce field-induced perpendicular vortices, then R would instead be proportional to B or depend exponentially on B . Also the observed R has an Arrhenius temperature dependence consistent with the hopping of spontaneous perpendicular vortices and not the motion of field-induced perpendicular vortices.

The MoGe microbridge of thickness $d = 50$ nm, width $w = 6$ μ m, and length $l = 102$ μ m was oriented so the B was parallel to the film plane and perpendicular to current I . The

film was sputtered onto a silicon substrate with a 200-nm-thick oxide layer using an alloy target of atomic composition $\text{Mo}_{0.79}\text{Ge}_{0.21}$. The deposition system had a base pressure of 2×10^{-7} Torr and the argon-gas working pressure was maintained at 3 mTorr during the sputtering. The growth rate was 0.15 nm/s. The film was patterned using photolithography and argon ion milling.

Our films had the following parameters which were measured independently: $T_c = 5.45$ K, $R_n = 540 \Omega$, $dB_{c2}/dT|_{T_c} = -3.13$ T/K, and $dI_d^{2/3}/dT|_{T_c} = -0.0119$ A $^{2/3}$ /K. Here R_n is the normal-state resistance at T_c and $I_d(T)$ is the depairing current near T_c . $B_{c2}(T)$, and, hence, ξ , were determined to high accuracy in our earlier work⁷ by fitting the entire resistive transition $R(T, B)$ to the flux flow theory rather than simply looking at T_c shifts at some resistive criterion such as $R = R_n/2$. The value of $I_d^{2/3}$ and, hence, λ were estimated by taking the T_c shifts at $R = R_n/2$, as described in detail in Ref. 9.

In this work we measured the voltage-current characteristics of the films in the Ginzburg-Landau (GL) region close to T_c , where $\lambda(t) = \lambda_0/\sqrt{1-t}$, $\xi(t) = \xi_0/\sqrt{1-t}$, $B_{c2}(T) = B_{c20}(1-t)$, $I_d(t) = I_{d0}(1-t)^{3/2}$, and $t = T/T_c$. Here $\lambda_0 = (\phi_0 d w / 3\sqrt{3}\pi\mu_0 I_{d0}\xi_0)^{1/2} = 646$ nm and $\xi_0 = (\Phi_0 / 2\pi B_{c20})^{1/2} = 4.39$ nm. The large GL parameter, $\kappa = \lambda_0/\xi_0 = 147$, indicates a very dirty film. The Pearl screening length $\Lambda(t) = 2\lambda^2(t)/d = 16.7/(1-t)$ μm well exceeds w for all T , so the sheet current density $J = I/w$ is uniform over the bridge width.

Our previous reviews and other papers⁷⁻¹⁰ give further details about the measurement technique, thermal analysis, and parameter determination.

III. EXPERIMENTAL RESULTS AND DISCUSSION

Figure 1 shows the temperature dependence of resistance observed at various magnetic fields. Each panel corresponds to a different fixed current. At lower B and I , there is some kind of transition temperature T_v (marked by the arrows) at which the $R(T)$ curves converge and plunge to zero. Notice that the transition becomes less sharply defined as I and B are increased. In the limit of low I and B , $T_v \simeq 4.7$ K. There is a qualitative difference in the transport response above and below T_v . At $T > T_v$ a finite resistance was always observed: an Ohmic response at low currents that becomes nonlinear at high I [Fig. 2(a)]. Below T_v , R we observed zero resistance up to a high value of I on the order of I_d at which an abrupt transition to the normal state occurred.

The lower two panels of Fig. 2 show the dependence of R on the angle between the applied B and the film plane. For $T < T_v$, there is an $R = 0$ plateau of angular width corresponding to the tilt $\pm 2d/w \approx \pm 1^\circ$ that causes the vortex to emerge outside the thickness; for $T > T_v$, we have $R \neq 0$ even at $\theta = 0$ because of dissipation from spontaneous perpendicular vortices generated by thermal fluctuations. As discussed in the previous section, the angular dependence in this resistive regime allows the $\theta = 0$ alignment to be verified to high accuracy.

It turns out that the observed T_v is rather close to the core explosion temperature T_v defined by $d = 4.4\xi(T_v)$.² Indeed, for $\xi(T_v \simeq 4.7\text{K}) = 11.8$ nm, we obtain $4.4\xi = 52$ nm, which

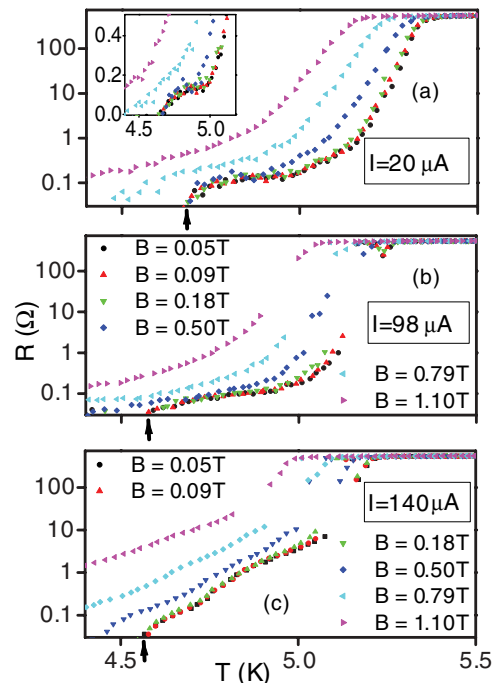


FIG. 1. (Color online) Resistive transitions in various indicated parallel magnetic fields and applied currents. There is a transition temperature T_v (indicated by arrows) at which the $R(T)$ curves at low B converge and plunge to zero. B values of different symbols are indicated in panels (b) and (c). The inset of panel (a) shows its data plotted with linear axes for R as well as T .

is remarkably close to the film thickness $d = 50$ nm. Phase transitions of the vortex matter (liquid-to-solid or liquid-to-glass) can also cause sharp drops in $R(T)$,¹¹ but in the field range of our measurements there can be no more than one row of vortices in our films. Indeed, using the London expression for B_{c1}^{\parallel} in which the vortex core energy is included,⁶ we obtain $B_{c1}^{\parallel}(4.7\text{K}) = (2\phi_0/\pi d^2)[\ln(d/\xi) - 0.07] = 0.72$ T, well above the lowest magnetic fields at which the resistive transition at T_v was observed. This estimate of B_{c1}^{\parallel} may not be very reliable for a film with $d \simeq 4\xi$, although more accurate calculations of vortices in thin films in the GL theory have been done.^{4,5} Yet the London model suggests that the films ought to be in the Meissner state at the lowest fields $B \simeq 0.05\text{--}0.1$ T of our measurements for which the sharpest resistive transition at T_v was observed. Therefore, the motion of parallel vortices cannot explain the resistance for $T > T_v$, suggesting a transition to a resistive state in which short perpendicular vortices generated by thermal fluctuations hop across the film width.

The data above indicate that the film is in the Meissner state for $T < T_v$ and that the resistive state above T_v may arise from thermally activated hopping of short perpendicular vortices generated by thermal fluctuations. In this case the I - V characteristic for uncorrelated hopping of single vortices across the film of width $w < \Lambda$ and thickness $d \ll w$ was obtained Ref. 6. In the case of zero perpendicular magnetic field the V - I characteristics is given by⁶

$$V = \frac{2IR_n(\beta - 1)}{\gamma\Gamma(\beta + 1)} \left[\frac{2\pi\xi}{w} \right]^\beta \left| \Gamma\left(1 + \frac{\beta}{2} + i\gamma\right) \right|^2 \sinh \pi\gamma, \quad (1)$$

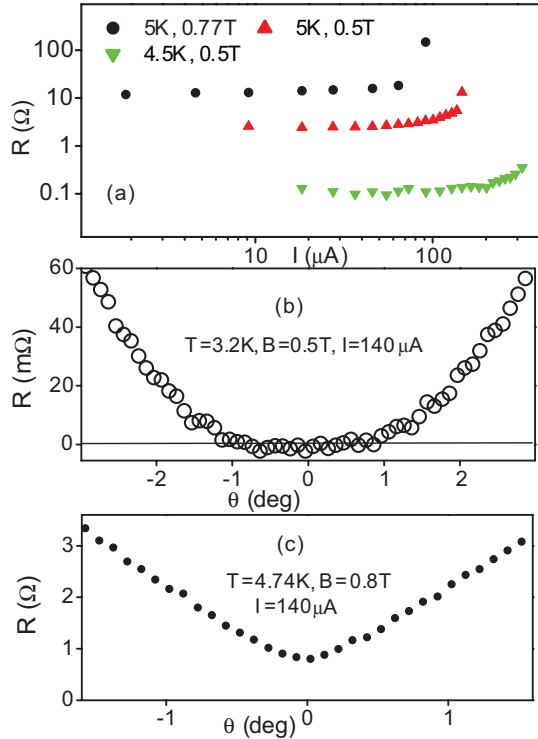


FIG. 2. (Color online) (a) Resistance versus current curves for a few temperatures and fields above T_v . The response is Ohmic at low I turning nonlinear at high I . [(b) and (c)] Angular dependence of resistance at fixed T , B , and $I = 140 \mu\text{A}$. (b) Below T_v there is an $R = 0$ plateau for the angular range $\sim \pm 2d/w \approx \pm 1^\circ$ within which the applied $\parallel B$ does not generate \perp vortices. (c) Above T_v , $R \neq 0$ for all I and B because of the hopping of edge nucleated \perp vortices.

where $\beta = \epsilon/T$, $\epsilon = d\phi_0^2/4\pi\mu_0\lambda^2$, $\gamma = \phi_0 I/2\pi T$, and $\Gamma(x)$ is the gamma function. Equation (1) gives an Ohmic $V(I) = R_v I$ at $I < I^*\xi/w$ and a power-law $V(I)$ at $I^*\xi/w \ll I < I^*$, consistent with the observed behavior of $V(I, T, V)$ shown in Figs. 1 and 2(a). Here $I^* = w\phi_0/2\pi e\Lambda\xi$ is of the order of the depairing current. The asymptotic expressions for the resistance $R = V/I$ in these current domains are

$$R(I) \simeq \sqrt{2\pi\beta}(I/I^*)^\beta R_n, \quad I^*\xi/w \ll I < I^* \quad (2)$$

$$R_v \simeq \sqrt{2}R_n(\pi\beta)^{3/2}(\xi/w)^\beta, \quad I < I^*\xi/w. \quad (3)$$

In the GL region $\beta(t) = \beta_0(1-t)/t$ with the Arrhenius parameter $\beta_0 = \phi_0^2 d/4\pi\mu_0\lambda_0^2 k_B T_c \approx 436$, and $I^*(t) = I_0^*(1-t)^{3/2}$ with $I_0^* = \phi_0 d w/4\pi\mu_0 e \lambda_0^2 \xi_0 \approx 7.9 \text{ mA}$.

Before using Eq. (1) to describe our experimental data, we estimate the range of temperatures $T_{\text{BKT}} < T < T_c$ of the BKT pair dissociation, where T_{BKT} is defined by the equation $\epsilon(T_{\text{BKT}}) = 2k_B T_{\text{BKT}}$. Using the parameters of our films presented above, we obtain that the BKT region $T_c - T_{\text{BKT}} = 2T_c/(2 + \beta_0) \approx 0.025 \text{ K}$ is very close to T_c and is much narrower than the temperature range of our measurements.

A parallel B does not influence the dynamics of perpendicular vortices in the London theory used to obtain Eqs. (1)–(3). However, the GL pairbreaking of Meissner screening currents flowing parallel to the film cause a variation in the large Arrhenius parameter $\beta(T) = U/T$, which in turn leads

to a strong B dependence of $R(T, B) \propto \exp(-U/T)$. The activation barrier $U(T)$ is due to the variation of the self-energy of the vortex across the film. The Meissner currents reduce the superfluid density $n_s(B) = n_s \int_{-d/2}^{d/2} (1 - Q^2 \xi^2) dx/d$ averaged over the film thickness, where $Q = 2\pi Bx/\phi_0$ is the gauge-invariant phase gradient of the order parameter.¹² Thus, $n_s(B) = [1 - (\pi\xi dB/\phi_0)^2/3]$ decreases quadratically with B . Taking into account the gradient terms in the GL equation and assuming no suppression of the order parameter at the film surface, we obtain a more accurate quadratic field correction in $\beta(B)$:

$$\beta(B) = \beta_0[1 - (B/B^*)^2](1-t)/t, \quad B \ll B^* \quad (4)$$

$$B^* = \sqrt{3}\phi_0/\pi\xi\sqrt{12\xi^2 + d^2}. \quad (5)$$

Here $B^*(T)$ is linear in T at $T_c - T < 12T_c(\xi_0/d)^2$ and exhibits a square-root temperature dependence $B^* \sim \phi_0/d\xi \propto \sqrt{T_c - T}$ at lower temperatures $T_c - T > 12T_c(\xi_0/d)^2 \simeq 0.5 \text{ K}$ for our films. Equations (2) and (4) predict an exponential dependence of $R(B)$ on B^2 :

$$t \frac{\ln(R_n/R)}{\beta_0 \ln(I_0^*/I)} = 1 - t - \frac{B^2}{B_0^2} \left[1 + \frac{\alpha}{1-t} \right], \quad (6)$$

where $B_0 = \sqrt{3}\phi_0/\pi\xi_0 d$ and $\alpha = 12(\xi_0/d)^2 \approx 0.093$. From Eq. (6) and in reference to the resistive transition curves of Fig. 1, we define a ‘‘critical temperature’’ $T_R(R_c, B, I) = t_R T_c$ at which $R(T, B, I)$ reaches a certain value R_c for given B and I . For $t < 1 - \alpha$ (which holds for $R < 10\Omega$) the last term in the brackets can be neglected, and Eq. (6) gives $B = B_0\sqrt{1 - t_R f}$, where $f = 1 + \ln(R_n/R_c)/\{\beta_0 \ln(I_0^*/I)\} \approx 1$. Hence,

$$T_R \simeq T_c(1 - B^2/B_0^2)/f. \quad (7)$$

Equation (7) shows that T_R declines linearly with B^2 with a slope $-T_c/fB_0^2 \approx -T_c/B_0^2 = -0.22$. This estimate is consistent with the average experimental slope of -0.29 inferred from the plots of the measured T_R (values of T where the curves in Fig. 1 attain 1- Ω and 3- Ω resistance values) at the respective applied B fields shown in Fig. 3(a). Equation (3) and (4) give the exponential dependence of the Ohmic resistance R_v on B^2 :

$$\frac{d \ln R}{dB^2} = \frac{\beta_0}{tB_0^2} \left[1 + \frac{\alpha}{1-t} \right] \ln \frac{w}{\xi(t)}. \quad (8)$$

Figure 3(c) shows that the experimental Ohmic resistance indeed varies exponentially with B^2 with a slope increasing with T . (Note that if the perpendicular vortices were simply created by a misalignment of the applied field, then R would have been proportional to B instead of the B^2 dependence that comes from the mechanism we discussed.) For the parameters of our films Eq. (8) gives $d \ln R_v/dB^2$ about 10–12 times greater than the observed values, mostly because of the factor $\ln(w/\xi) \simeq 10$ in Eq. (8). One reason for this discrepancy may be the material uncertainty in β_0 resulting from possible suppression of superconductivity at the film surface and substrate. The superfluid density can then vary across the film even in the absence of the parallel magnetic field. This effect is particularly pronounced at $T \approx T_c$, where $d < 2\xi(T)$ so any suppression of superconductivity at the surface propagates all the way across the film. To circumvent this uncertainty, we

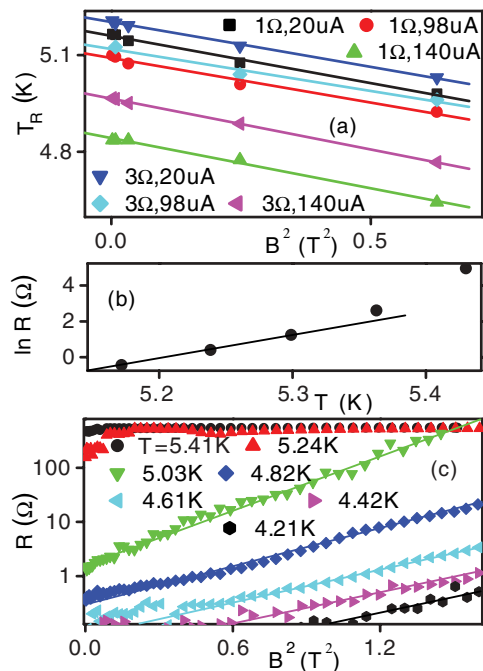


FIG. 3. (Color online) (a) Plots of T_R versus B^2 for the indicated resistance criteria and currents. $T_R(R_c, B, I)$ is defined as the value of T where $R = R_c$ on the curves in Fig. 1, for the given I and B . (b) Resistive transition at $I = 13 \mu A$ and $B = 0$ used to obtain the zero-field logarithmic slope S . (c) The Ohmic resistance [at $I = 27 \mu A$ in the middle of the Ohmic current range as per Fig. 2(a)] shows an exponential dependence on B^2 . Different curves are at indicated temperatures.

use Eq. (3) to express β_0 in terms of the measured zero-field slope $S = d \ln R / dt \simeq (\beta_0 / t^2) \ln(w / \xi)$ at $B = 0$, shown in Fig. 3(b). Substituting S into Eq. (8) yields $d \ln R_v / dB^2$ in terms of measured parameters:

$$\frac{d \ln R}{dB^2} = \frac{St}{B_0^2} \left[1 + \frac{\alpha}{1-t} \right]. \quad (9)$$

For $S = 70.3$ inferred from the $\ln R$ vs. T data shown in Fig. 3(b), Eq. (9) gives $d \ln R / dB^2 = 2.83, 3.14, 3.52, 4.14,$ and $5.28 T^{-2}$ at $T = 4.21, 4.42, 4.61, 4.82,$ and 5.03 K, respectively. These are in agreement within a factor of 1.5 with the measured slopes of Fig. 3(c): 2.19, 2.21, 2.32, 2.69, and $3.85 T^{-2}$.

These results indicate that the resistive state above T_v is consistent with thermally activated hopping of spontaneous perpendicular vortices tuned by the parallel magnetic field. Some of the quantitative discrepancy with experiment may arise from randomly distributed pinning centers, which provide shorter hopping distances $\ell \ll w$. Pinning centers in a film of thickness $d \sim \xi$ locally reduce the energy of a vortex by $\alpha\epsilon$ where ϵ is the core energy and $\alpha < 1$ depends on the details of pinning interaction.¹¹ The drift velocity of the vortex $\bar{v} \sim \ell / \tau$ is then limited by the mean hopping time $\tau \propto \exp(\alpha\epsilon / T)$ leading to a much higher Ohmic resistance $R_v \sim R_0 \exp(-\alpha\epsilon / T)$ as compared to Eq. (3) which implies hopping of a vortex across the entire film width. Using $\alpha\epsilon$ instead of $\epsilon \ln(w / \xi)$ in Eq. (8) significantly reduces $d \ln R_v / dB^2$, in agreement with experiment. In turn, pinning

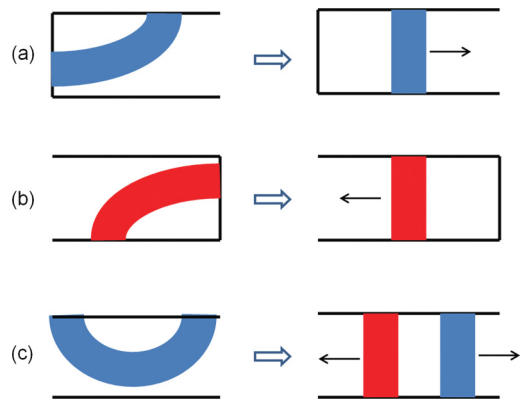


FIG. 4. (Color online) A sketch of vortex segments nucleated by thermal fluctuations at the edge of the film (a) and (b) and on the broad face of the film (c).

becomes less essential for the nonlinear part of the I - V curve where the activation barrier $U = \epsilon \ln(I_*/I)$ is not only much reduced but also localized in a narrow ($\ll w$) region at the film edge.⁶ As a result, Eqs. (6) and (7) describe the experimental data well at high currents.

A possible mechanism by which the core explosion of parallel vortices could facilitate nucleation of perpendicular vortices is illustrated by Fig. 4. There are three different possibilities: vortex quarter-loops of different polarities nucleate at the film edges [Figs. 4(a) and 4(b)] or vortex semiloops nucleate at the broad face of the film [Fig. 4(c)]. Because the normal component of circulating vortex current vanishes at the film surface, the energy U_{ql} of the vortex quarter-loops at the edges is exactly half of the energy of the face semiloop $U_{sl} = 2U_{ql}$ which can be regarded as two quarter-loops with opposite polarity. At low temperatures the edge quarter-loops will therefore dominate the thermally activated voltage $V \propto \exp[-U_{ql} / k_B T]$ despite smaller statistical weight of edge nucleation as compared to the semiloop nucleation on the broad face of the film. As temperature increases, particularly at T close to T_{BKT} , the semiloop nucleation takes over and V is determined by the BKT pair dissociation. In thin films with $d < 4.4\xi$, the segments of vortex semiloops or quarter-loops parallel to the broad face of the film are unstable and quickly propagate across the film. As a result, the edge semiloops turn into either short perpendicular vortices [Fig. 4(a)] or antivortices [Fig. 4(b)] which are then driven by a transport current across the film. The expansion of the vortex semiloop in Fig. 4(c) turns it into a vortex-antivortex pair which is then driven apart by the current. This process is a part of the BKT pair dissociation. Detailed calculations of these processes requires numerical simulation of the 3D Ginzburg-Landau equations (see, e.g., Ref. 5).

IV. CONCLUSION

To summarize, our magnetotransport measurements in a thin MoGe film in a parallel magnetic field revealed a thermal fluctuation-driven transition to a dissipative state caused by the motion of thermally activated perpendicular vortices. This results in the Arrhenius V - I characteristics which have been observed in several decades in voltage. It appears that the observed transition temperature T_v matches the vortex

explosion condition of $d = 4.4\xi(T)$. We showed that the resistive state above T_v can be tuned by the pairbreaking effect of the parallel field. The suppression of the sheet superfluid density by the parallel field can also be used to tune the V - I characteristics of thin superconducting films in the BKT temperature region.

ACKNOWLEDGMENTS

The authors gratefully acknowledge Jiong Hua, Zhili Xiao, James M. Knight, and Richard A. Webb. This work was supported by the US Department of Energy through Grant No. DE-FG02-99ER45763.

*Corresponding author: kunchur@sc.edu; [<http://www.physics.sc.edu/kunchur>].

¹A. A. Abrikosov, Zh. Eksp. Teor. Fiz. **46**, 1464 (1964) [Sov. Phys. JETP **19**, 988 (1964)].

²K. K. Likharev, *Rev. Mod. Phys.* **51**, 101 (1979).

³S. H. Brongersma, E. Verweij, N. J. Koeman, D. G. deGroot, R. Griessen, and B. I. Ivlev, *Phys. Rev. Lett.* **71**, 2319 (1993); A. Geim *et al.*, *Nature* **390**, 259 (1997); G. Stan, S. B. Field, and J. M. Martinis, *Phys. Rev. Lett.* **92**, 097003 (2004); V. R. Misko, V. M. Fomin, J. T. Devreese, and V. V. Moshchalkov, *ibid.* **90**, 147003 (2003)

⁴P. Sánchez-Lotero and J. J. Palacios, *Phys. Rev. B* **75**, 214505 (2007); V. N. Gladilin, J. Tempere, J. T. Devreese, W. Gillijns, and V. V. Moshchalkov, *ibid.* **80**, 054503 (2009); B. J. Baelus, A. Kanda,

N. Shimizu, K. Tadano, Y. Ootuka, K. Kadowaki, and F. M. Peeters, *ibid.* **73**, 024514 (2006).

⁵C. Qiu and T. Qian, *Phys. Rev. B* **77**, 174517 (2008); D. Yu. Vodolazov, *ibid.* **85**, 174507 (2012).

⁶A. Gurevich and V. M. Vinokur, *Phys. Rev. Lett.* **100**, 227007 (2008).

⁷M. Liang, M. N. Kunchur, J. Hua, and Z. Xiao, *Phys. Rev. B* **82**, 064502 (2010).

⁸M. Liang and M. N. Kunchur, *Phys. Rev. B* **82**, 144517 (2010).

⁹M. N. Kunchur, *J. Phys.: Condens. Matter* **16**, R1183 (2004).

¹⁰M. N. Kunchur, *Mod. Phys. Lett. B* **9**, 399 (1995).

¹¹G. Blatter *et al.*, *Rev. Mod. Phys.* **66**, 1125 (1994).

¹²N. Groll, A. Gurevich, and I. Chiorescu, *Phys. Rev. B* **81**, 020504(R) (2010).